Acta Mechanica 136, 91 – 107 (1999)

ACTA MECHANICA

On the effects of microstress on macroscopic diffusion processes

T. I. Zohdi and **P. Wriggers,** Hannover, Germany

Dedicated to Prof. Dr. Peter Haupt on the occasion of his 60th birthday

(Received February 19, 1998; revised March 25, 1998)

Summary. The effects of internal microstress fields are neglected in a usual simulation of the diffusion of a small solute trough solid heterogeneous media. However, when a heterogeneous material is used in a structure undergoing external mechanical loading, highly nonuniform stress fields can arise locally due to the variable microstructure. In this paper a simple quasi-Fickian model is studied which employs a spatially variable stress-dependent diffusivity, $\boldsymbol{D}^{\sigma}$. The structure of $\boldsymbol{D}^{\sigma}$ stems from an assumption that the stresses nonuniformly open and close the pores of the material microstructure, thus providing preferential sites for accumulation of the diffusing solute. When $\boldsymbol{\sigma}= 0$, the usual stress-free Fickian diffusivity, $\boldsymbol{D}^{0}$, is recovered. Because of the highly oscillatory stress fields on the micro level, when employing numerical methods, such as the finite element or finite difference method, the distance between discretization nodes must be far smaller than the microstructural oscillations to obtain accurate simulations. This fact makes direct numerical simulations involving $\boldsymbol{D}^{\sigma}$ virtually impossible without computationally intensive, and complicated, special techniques. In this paper upper bounds are developed for the difference between solutions produced when using $\boldsymbol{D}^{\sigma}$ and alternatively $\boldsymbol{D}^{0}$ in the body under analysis. The general case, when $\boldsymbol{D}^{0}$, $\boldsymbol{\sigma}$ and consequently $\boldsymbol{D}^{\sigma}$, are spatially variable, is considered. The bounds are a function of only $\boldsymbol{D}^{0}$ and σ *and do not require any knowledge of the stress-dependent solution,* and can thus be used as an a-priori check to determine whether potentially expensive computations are necessary.

1 Introduction and Motivation

There are a variety of structural analyses where an important issue is the diffusive behavior of a small solute through a body in the presence of nonuniform stress fields. In many instances, the determination of such diffusive behavior is critical to the estimation of the useful service life of solid structures in contact with corrosive environments. An important example is the absorption and accumulation of potentially hazardous solutes, such as hydrogen. Hydrogen, due to its relatively small atomic structure, easily diffuses through most materials, and its absorption can result in a variety of structural failures at loading levels significantly lower than those predicted under hydrogen-free conditions. There are many forms of hydrogen damage. A common form is hydrogen embrittlement, which is a mechanical-environmental failure phenomena that results from the excessive absorption of hydrogen usually due to residual or applied stresses. Typically, hydrogen is introduced in materials in atomic form (H) either electrolytically or from a gaseous atmosphere as a product of corrosion or a waste product in combustion cycles. The primary effects are subcritical crack growth at loading levels

far below those associated with unstable (hydrogen-free) crack motion. A wide variety of materials, conventional materials, advanced alloys, intermetallics and ceramics, are susceptible to hydrogen embrittlement. Cracking caused by this process is often referred to as hydrogen-stress cracking or hydrogen-induced cracking. It has been suggested in the literature that cracking in such materials occurs because hydrogen absorption at these sites lowers the surface energy required for cracks to grow. Loosely speaking, hydrogen sufficiently reduces the bonding energy of the metal lattice enough to allow cracking and, in some cases, enhances localized plastic deformation. For indepth studies of this topic, from a materials science point of view, see [1] or [2]. For a review of the state-of-the-art of continuum modeling of hydrogen-assisted failure we refer the reader to the recent work in [3]. For industrial case studies of structural failures due to the presence of hydrogen and mechanical stress, we refer the reader to the official publication of the American Society for Metals [4]. Obviously, hydrogen diffusion is only one of many examples where the behavior of a small solute is affected by the presence of stress. Other cases include moisture swelling in polymers, hydration of concrete and soil saturation.

In many cases, either naturally or by design, a solid medium through which a solute diffuses contains heterogeneities on the microscale. In these cases, it is usually assumed that the diffusivity is insensitive to the effects of stress. However, it is clear that if there are large phase contrasts in the elastic properties, then local stress fields may be large in magnitude and highly nonuniform, and thus the effects of stress may be important. In this paper a simple quasi-Fickian model is studied which employs a spatially variable stress-dependent diffusivity, $\boldsymbol{D}^{\sigma}$, where $\boldsymbol{\sigma}$ is the stress at a point. The structure of $\boldsymbol{D}^{\sigma}$, which we leave general at this point in the presentation, stems from an assumption that the nonuniform microstresses locally open and close the pores of the material microstructure, thus providing preferential sites for accumulation of the diffusing solute. When $\sigma = \mathbf{0}$, then the usual stress-free diffusivity, $\boldsymbol{D}^{0}$, is recovered. Because of the highly variable stress fields on the micro level $\boldsymbol{D}^{\sigma}$ will also be highly oscillatory. Consequently, when employing $\boldsymbol{D}^{\sigma}$, standard numerical methods, such as the finite element or finite difference method, require the distance between discretization nodes to be far smaller than the microstructural oscillations to obtain accurate simulations. This fact makes the usual direct numerical simulations involving $\boldsymbol{D}^{\sigma}$ virtually impossible without computationally intensive, and complicated, special techniques. In many cases it is unclear whether such computations are necessary. In order to determine whether such expensive computations are indeed justified, the main focus of the paper is to bound the deviation of the stress-dependent solution (using $\boldsymbol{D}^{\sigma}$) and the stress-free solution (using $\boldsymbol{D}^{0}$), in an a priori manner, in terms of only the inexpensive stress-free solution and the physical data. The general case where $\boldsymbol{D}^{0}$, $\boldsymbol{\sigma}$ and consequently $\boldsymbol{D}^{\sigma}$, are spatially variable is considered. The bounds are shown to be optimal, i.e. they can attain equality under certain conditions. Several examples are given to illustrate the predicted differences between stress-dependent and stress-free solution behavior.

The paper outline is as follows. In Sect. 2 the model and governing equations are introduced. In Sect. 3 general a priori bounds on the difference between solutions for the stress-free and stress-dependent cases are developed, in terms of the stress field and the stress-free diffusivity. The bounds are shown to be sharp, i.e. they can attain equality. In Sect. 4 the relationship is investigated between the bounds on the difference in the solution and classical notions of effective diffusivity bounds. In Sect. 5 examples are presented which illustrate the effects of stress and the predicted differences between the stress-dependent and stress-free solutions. Finally, in Sect. 6 a summary is given.

2 The basic model

There has been an enormous amount of research dealing with diffusion, or relatedly, heat conduction which deviate from the classical models of Fick and Fourier. Works dating back, at least, to Maxwell [5] have postulated models which deviate from such models. Rather than attempt to catalog the various models in the literature, and arguments to justify them, we refer the reader to the encyclopedic survey article of Joseph and Preziosi [6], which gives a chronology of virtually all nonstandard models from that of Maxwell through to 1989. Also other reviews which deal with related material, in particular multi-field coupling, can be found in [7]–[10]. Generally speaking, most approaches have sought to modify the standard model by introducing terms representing possibly important effects neglected in the classical approaches of Fick and Fourier. In this vein, models for stress-dependent diffusion in solid media can be found in the literature. We refer the reader to the classical work of Crank [11] which reviews a variety of models and also to specific works dealing with hydrogen diffusion, [12]–[16].

2.1 Direct incorporation of stress-dependency

The most obvious, and simplest, approach to incorporate stress-dependency is to postulate a stress-dependent diffusivity ([17], [18])

$$\mathcal{F} = -\boldsymbol{D}^{\sigma} \cdot \nabla c^{\sigma},$$

where

$$\boldsymbol{D}^{0} \stackrel{\text{def}}{=} \boldsymbol{D}^{\sigma=0}, \tag{1}$$

where c^{σ} is the concentration of the solute, $\boldsymbol{\sigma}$ is the stress present at a point, and $\boldsymbol{D}^{\sigma}$ is a positive definite, second order tensorial function of position. $\boldsymbol{D}^{0}$ is the stress-free diffusivity. Upon substituting the equation corresponding to this model into the conservation law, $\dot{c}^{\sigma} + \nabla \cdot \mathcal{F}^{\sigma} = 0$, one obtains the following equation describing the diffusion of a dilute solute in a stressed solid

$$\dot{c}^{\sigma} = \nabla \cdot (\boldsymbol{D}^{\sigma} \cdot \nabla c^{\sigma}). \tag{2}$$

For small species at dilute concentrations, one can consider a weak coupling where the applied mechanical stress field is not affected by the diffusing species. This is the only case considered in this paper. Observe that the equation is parabolic for the unsteady state, as is the classical diffusion equation based on the Fickian model, $\dot{c}^{\sigma=0} = \nabla \cdot (\boldsymbol{D}^{\sigma=0} \cdot \nabla c^{\sigma=0})$. As we have stated, our objective in this paper is to bound the differences in the solutions using $\boldsymbol{D}^{\sigma}$ and $\boldsymbol{D}^{0}$ in terms of $\boldsymbol{D}^{0}$ and $\boldsymbol{\sigma}$ (spatially variable), under steady state conditions ($\dot{c} = 0$).

2.2 Variational formulations

We consider a structure which occupies an open bounded domain in $\Omega \in \mathbb{R}^3$. Its boundary is denoted $\partial\Omega$. The body is in equilibrium ($\dot{c} = 0$) under the action of possible body source terms, $\boldsymbol{b}$, and surface fluxes, $\boldsymbol{f}$. The boundary $\partial\Omega$ consists of a portion Γ_c on which the concentrations, $c = d$, are prescribed, and a part Γ_f on which fluxes, $\mathcal{F} = -\boldsymbol{f}$, are prescribed.

2.2.1 The unstressed case

The unstressed diffusion solution, $c^0 \stackrel{\text{def}}{=} c^{\sigma=0}$, is characterized by the following variational formulation:

Find

$c^0 \in H^1(\Omega),\ c^0|_{\Gamma_c} = d,$

such that

$$\int_\Omega \nabla v \cdot \boldsymbol{D}^0 \cdot \nabla c^0 d\boldsymbol{x} = \int_\Omega bv\, d\boldsymbol{x} + \int_{\Gamma_f} \boldsymbol{f} \cdot \boldsymbol{n} v\, ds \qquad \forall v \in H^1(\Omega),\ v|_{\Gamma_c} = 0, \tag{3}$$

where $H^1(\Omega)$ is the Sobolev space of $L^2(\Omega)$ functions whose derivatives also lie in $L^2(\Omega)$. Here $\boldsymbol{D}^0$ is an arbitrary second rank linear diffusivity tensor with usual symmetries and positive definite character. The components of $\boldsymbol{D}^0$ are functions of spatial position in the body.

2.2.2 The stressed case

The stressed-dependent diffusion, c^σ, is characterized by the following variational formulation:

Find

$c^\sigma \in H^1(\Omega),\ c^\sigma|_{\Gamma_c} = d,$

such that

$$\int_\Omega \nabla v \cdot \boldsymbol{D}^\sigma \cdot \nabla c^\sigma\, d\boldsymbol{x} = \int_\Omega bv\, d\boldsymbol{x} + \int_{\Gamma_f} \boldsymbol{f} \cdot \boldsymbol{n} v\, ds \qquad \forall v \in H^1(\Omega),\ v|_{\Gamma_c} = 0. \tag{4}$$

Here we require $\boldsymbol{D}^\sigma$ to be a symmetric and positive definite tensor. This places restrictions on the dependence of $\boldsymbol{D}^\sigma$ on $\boldsymbol{\sigma}$. To keep the analysis general, we leave $\boldsymbol{D}^\sigma$ and $\boldsymbol{D}^0$ arbitrary but symmetric and positive definite. Specific choices are made later in the paper.

3 A general upper bound on the stress-dependent behavior

Since variational formulations are employed to generate the solutions the following associated semi-norm is used to measure their difference,

$$\|c^\sigma - c^0\|^2_{D^\sigma(\Omega)} \stackrel{\text{def}}{=} \int_\Omega (\nabla c^\sigma - \nabla c^0) \cdot \boldsymbol{D}^\sigma \cdot (\nabla c^\sigma - \nabla c^0)\, d\boldsymbol{x}. \tag{5}$$

However, in the event that concentrations are specified on the boundary, then $c^\sigma - c^0 = constant$ is unobtainable unless $c^\sigma - c^0 = 0$, and the semi-norm in Eq. (5) is a norm in the strict mathematical sense.

Our objective is to bound $\|c^\sigma - c^0\|_{D^\sigma(\Omega)}$ in terms of the data $\boldsymbol{D}^0$, $\boldsymbol{\sigma}$, and the stress-free solution c^0. By definition

$$\int_\Omega \nabla v \cdot \boldsymbol{D}^\sigma \cdot \nabla c^\sigma\, d\boldsymbol{x} = \int_\Omega \nabla v \cdot \boldsymbol{D}^0 \cdot \nabla c^0\, d\boldsymbol{x} = \int_\Omega bv\, d\boldsymbol{x} + \int_{\Gamma_f} \boldsymbol{f} \cdot \boldsymbol{n} v\, ds, \tag{6}$$

and subtracting $\int_\Omega \nabla v \cdot \boldsymbol{D}^\sigma \cdot \nabla c^0 \, d\boldsymbol{x}$ from both sides yields

$$\int_\Omega \nabla v \cdot \boldsymbol{D}^\sigma \cdot \nabla (c^\sigma - c^0) \, d\boldsymbol{x} = \int_\Omega \nabla v \cdot (\boldsymbol{D}^0 - \boldsymbol{D}^\sigma) \cdot \nabla c^0 \, d\boldsymbol{x}. \tag{7}$$

Since v is an arbitrary virtual displacement, we may set $v = c^\sigma - c^0$ to yield

$$\begin{aligned}
\|c^\sigma - c^0\|^2_{D^\sigma(\Omega)} &= \int_\Omega \nabla (c^\sigma - c^0) \cdot (\boldsymbol{D}^0 - \boldsymbol{D}^\sigma) \cdot \nabla c^0 \, d\boldsymbol{x} \\
&= \int_\Omega \nabla (c^\sigma - c^0) \cdot \boldsymbol{D}^\sigma \cdot \boldsymbol{D}^{\sigma-1} \cdot (\boldsymbol{D}^0 - \boldsymbol{D}^\sigma) \cdot \nabla c^0 \, d\boldsymbol{x} \\
&= \int_\Omega \boldsymbol{D}^{\sigma\frac{1}{2}} \cdot \nabla (c^\sigma - c^0) \cdot \boldsymbol{D}^{\sigma\frac{1}{2}} \cdot \boldsymbol{D}^{\sigma-1} \cdot (\boldsymbol{D}^0 - \boldsymbol{D}^\sigma) \cdot \nabla c^0 \, d\boldsymbol{x} \\
&\leq \underbrace{\sqrt{\left(\int_\Omega \nabla (c^\sigma - c^0) \cdot \boldsymbol{D}^\sigma \cdot \nabla (c^\sigma - c^0) \, d\boldsymbol{x}\right)}}_{\|c^\sigma - c^0\|_{D^\sigma(\Omega)}} \\
&\quad \times \sqrt{\left(\int_\Omega (\boldsymbol{D}^0 - \boldsymbol{D}^\sigma) \cdot \nabla c^0 \cdot \boldsymbol{D}^{\sigma-1} \cdot (\boldsymbol{D}^0 - \boldsymbol{D}^\sigma) \cdot \nabla c^0 \, d\boldsymbol{x}\right)},
\end{aligned} \tag{8}$$

where $\boldsymbol{D}^{\sigma\frac{1}{2}} \stackrel{\text{def}}{=} (\boldsymbol{D}^\sigma)^{\frac{1}{2}}$ and $\boldsymbol{D}^{\sigma-1} \stackrel{\text{def}}{=} (\boldsymbol{D}^\sigma)^{-1}$. Therefore

$$\|c^\sigma - c^0\|^2_{D^\sigma(\Omega)} \leq \int_\Omega (\boldsymbol{D}^0 - \boldsymbol{D}^\sigma) \cdot \nabla c^0 \cdot \boldsymbol{D}^{\sigma-1} \cdot (\boldsymbol{D}^0 - \boldsymbol{D}^\sigma) \cdot \nabla c^0 \, d\boldsymbol{x} \stackrel{\text{def}}{=} \mathcal{B}^2_{(\sigma-0)}. \tag{9}$$

It is emphasized that this relation holds for general loading, external geometry and nonconstant, anisotropic $\boldsymbol{D}^0$ *and* $\boldsymbol{D}^\sigma$. At this point in the presentation the stress field is arbitrary, and can be thought of as a parameter.

Example. If we consider a one dimensional structure of unit length, with a fixed concentration $c(0) = 0$ and $dc(1)/dx = G$, an arbitrary constant. The stress-dependent and unstressed problems are

$$\frac{d}{dx}\left(D^\sigma \frac{dc^\sigma}{dx}\right) = 0 \qquad \textit{and} \qquad \frac{d}{dx}\left(D^0 \frac{dc^0}{dx}\right) = 0. \tag{10}$$

Since $dc^\sigma/dx = G/D^\sigma$ and $dc^0/dx = G/D^0$, we have

$$\mathcal{B}^2_{(\sigma-0)} = \int_0^1 \left(\frac{G}{D^0}\right)^2 (D^0 - D^\sigma)^2 \frac{1}{D^\sigma} \, dx = G^2 \int_0^1 \left(\frac{1}{D^0} - \frac{1}{D^\sigma}\right)^2 D^\sigma \, dx = \|c^\sigma - c^0\|^2_{D^\sigma(\Omega)}. \tag{11}$$

In other words, the bound for the error in the solution is exact, regardless of the stress field. If we change the second boundary condition to $c(1) = K$, an arbitrary constant, then after some simple algebraic manipulations we have

$$\frac{\mathcal{B}^2_{(\sigma-0)}}{\|c^\sigma - c^0\|^2_{D^\sigma(\Omega)}} = \frac{\displaystyle\int_0^1 \left(\frac{1}{D^0} - \frac{1}{D^\sigma}\right)^2 D^\sigma \, dx}{\displaystyle\int_0^1 \left(\frac{1}{D^0} - \frac{1}{D^\sigma}\frac{\left\langle \frac{1}{D^0} \right\rangle}{\left\langle \frac{1}{D^\sigma} \right\rangle}\right)^2 D^\sigma \, dx}; \qquad \textit{where } \langle\cdot\rangle \stackrel{\text{def}}{=} \frac{1}{|\Omega|}\int_\Omega \cdot \, dx. \tag{12}$$

It is clear that the proximity of $\langle 1/D^0 \rangle$ to $\langle 1/D^\sigma \rangle$ governs the quality of the prediction in this case. We now focus on the relation of the solution bound to the classical theory of effective properties.

4 Stress-dependent effective properties

The computation of effective properties of heterogeneous materials involves the solution of boundary value problems posed over statistically representative volume element domains. In many cases such simulations are computationally quite complex and it is advantageous to bound the possible aggregate behavior a priori in terms of the physical data at hand. The study of effective properties has had a long history. Because the equation structure for elastostatics, thermal conductivity and diffusion are essentially identical in the linear regime, most of the various techniques for computing approximate effective elastic, thermal or diffusive properties, transfer easily from one regime to another. For a concise summary see [19]. Here we briefly review the basic concepts for linear elasticity, then apply and relate them to the $\mathcal{B}_{(\sigma-0)}$-bound.

4.1 The Hill-Reuss-Voigt bounds

In order to determine an effective macroscopic linear elasticity tensor, $\boldsymbol{E}^*$, a relation between averages, $\langle \boldsymbol{\sigma} \rangle = \boldsymbol{E}^* : \langle \boldsymbol{\varepsilon} \rangle$, must be computed, where $\langle \cdot \rangle \stackrel{\text{def}}{=} \frac{1}{|\Omega|} \int_{\Omega} \cdot \, d\boldsymbol{x}$, and where $\boldsymbol{\sigma}$ and $\boldsymbol{\varepsilon}$ are the stress and strain fields within a statistically representative volume element (RVE) with volume $|\Omega|$. Loosely speaking, an RVE is a theoretical structure small enough to be considered as a material point with respect to the size of the domain under analysis, but large enough to be a stratistically representative sample of the microstructure. Tacitly it is assumed that at least one choice of the RVE is possible. It is possible, under certain assumptions, to relate $\boldsymbol{E}^*$ to the approximations $\langle \boldsymbol{E} \rangle$, $\langle \boldsymbol{E}^{-1} \rangle^{-1}$ due to Voigt and Reuss respectively. The former, introduced in 1889 [20], is based on the assumptions of uniform strain throughout the body, the latter, introduced in 1929 [21], is based on the assumption of uniform stress. Hill, in 1952 [22] proved that

$$\underbrace{\langle \boldsymbol{\sigma} : \boldsymbol{\varepsilon} \rangle}_{\text{micro energy}} = \underbrace{\langle \boldsymbol{\sigma} \rangle : \langle \boldsymbol{\varepsilon} \rangle}_{\text{macro energy}} \Longrightarrow \underbrace{\langle \boldsymbol{E}^{-1} \rangle^{-1}}_{\text{Reuss}} \leq \boldsymbol{E}^* \leq \underbrace{\langle \boldsymbol{E} \rangle}_{\text{Voigt}}, \tag{13}$$

where this inequality means that the eigenvalues of the tensors $\boldsymbol{E}^* - \langle \boldsymbol{E}^{-1} \rangle^{-1}$ and $\langle \boldsymbol{E} \rangle - \boldsymbol{E}^*$ are nonnegative. The preceding ideas apply trivially to determine bounds on stress-dependent effective properties. In order to determine an effective macroscopic linear diffusivity tensor, $\boldsymbol{D}^{\sigma *}$, a relation between averages, $\langle \mathcal{F}^{\sigma} \rangle = -\boldsymbol{D}^{\sigma *} \cdot \langle \nabla c^{\sigma} \rangle$, must be computed, where $\mathcal{F}^{\sigma}$ and ∇c^{σ} are the flux and concentration gradient fields within a statistically representative volume element (RVE) with volume $|\Omega|$. As in the elastic case, $\boldsymbol{D}^{\sigma *}$ is not a material property, i.e., it depends on the data. If $\langle \mathcal{F}^{\sigma} \rangle$ and $\langle \nabla c^{\sigma} \rangle$ are such that $\langle \mathcal{F}^{\sigma} \cdot \nabla c^{\sigma} \rangle = \langle \mathcal{F}^{\sigma} \rangle \cdot \langle \nabla c^{\sigma} \rangle$, then

$$\underbrace{\langle \boldsymbol{D}^{\sigma -1} \rangle^{-1}}_{\text{Reuss}} \leq \boldsymbol{D}^{\sigma *} \leq \underbrace{\langle \boldsymbol{D}^{\sigma} \rangle}_{\text{Voigt}}. \tag{14}$$

Obviously, these bounds are stress-dependent. Of course we also have bounds for the unstressed diffusivity in the absence of stress

$$\underbrace{\langle \boldsymbol{D}^{0 -1} \rangle^{-1}}_{\text{Reuss}} \leq \boldsymbol{D}^{0 *} \leq \underbrace{\langle \boldsymbol{D}^{0} \rangle}_{\text{Voigt}}. \tag{15}$$

To bound the deviation of the effective properties with stress, we immediately have:

$$\langle \boldsymbol{D}^{\sigma-1}\rangle^{-1} - \boldsymbol{D}^{0*} \leq \boldsymbol{D}^{\sigma*} - \boldsymbol{D}^{0*} \leq \langle \boldsymbol{D}^{\sigma}\rangle - \boldsymbol{D}^{0*}, \tag{16}$$

and therefore

$$\langle \boldsymbol{D}^{\sigma-1}\rangle^{-1} - \langle \boldsymbol{D}^{0}\rangle \leq \boldsymbol{D}^{\sigma*} - \boldsymbol{D}^{0*} \leq \langle \boldsymbol{D}^{\sigma}\rangle - \langle \boldsymbol{D}^{0-1}\rangle^{-1}. \tag{17}$$

These inequalities can be thought of as defining an effective property bandwidth.

4.2 Relationship between the $\mathcal{B}_{(\sigma-0)}$-bound and the HRV-bounds

The expression on the left in Eq. (13) is often referred as Hill's condition and can be realized in several ways. A special class of fields that conform to Hill's condition are those produced in bodies with applied boundary data of the following form: (1) pure displacements in the form $\boldsymbol{u}|_{\partial\Omega} = \mathcal{S}\cdot\boldsymbol{x}$ or (2) pure tractions in the form $\boldsymbol{t}|_{\partial\Omega} = \mathcal{T}\cdot\boldsymbol{n}$, where $\mathcal{S}$ and $\mathcal{T}$ are constant strain and stress tensors, respectively. For obvious reasons, these types of boundary conditions are known as "uniform." It can be easily shown that under uniform conditions, for case (1) $\langle\boldsymbol{\varepsilon}\rangle = \mathcal{S}$, and for case (2) $\langle\boldsymbol{\sigma}\rangle = \mathcal{T}$ (with no body forces). Here we consider the analogous uniform concentration loadings, either $c|_{\partial\Omega} = \boldsymbol{K}\cdot\boldsymbol{x}$, where $\boldsymbol{K}$ is a constant concentration gradient or $\boldsymbol{f}|_{\partial\Omega} = \boldsymbol{G}$, where $\boldsymbol{G}$ is a constant concentration flux vector. These conditions satisfy Hill's conditions for the diffusion problem, regardless of the state of stress.

Uniform conditions. If the concentration loading is uniform and $\boldsymbol{D}^0$ is constant, then

$$\begin{aligned}\|c^{\sigma} - c^{0}\|^2_{D^{\sigma}(\Omega)} &\leq \int_{\Omega} (\boldsymbol{D}^0 - \boldsymbol{D}^{\sigma})\cdot\nabla c^0\cdot\boldsymbol{D}^{\sigma-1}\cdot(\boldsymbol{D}^0 - \boldsymbol{D}^{\sigma})\cdot\nabla c^0\, d\boldsymbol{x}\\ &= \int_{\Omega} (\nabla c^0\cdot\boldsymbol{D}^{\sigma}\cdot\nabla c^0 - 2\nabla c^0\cdot\boldsymbol{D}^0\cdot\nabla c^0 + \boldsymbol{D}^{\sigma-1}\cdot\boldsymbol{D}^0\cdot\nabla c^0\cdot\boldsymbol{D}^0\cdot\nabla c^0)\, d\boldsymbol{x}\\ &= \nabla c^0\cdot\langle\boldsymbol{D}^{\sigma}\rangle\cdot\nabla c^0\,|\Omega| - 2\nabla c^0\cdot\boldsymbol{D}^0\cdot\nabla c^0\,|\Omega|\\ &\quad + \langle\boldsymbol{D}^{\sigma-1}\rangle\cdot\boldsymbol{D}^0\cdot\nabla c^0\cdot\boldsymbol{D}^0\cdot\nabla c^0\,|\Omega|\end{aligned} \tag{18}$$

This can be compactly written as

$$\|c^{\sigma} - c^{0}\|^2_{D^{\sigma}(\Omega)} \leq \nabla c^0\cdot\left(\langle\boldsymbol{D}^{\sigma}\rangle + \boldsymbol{D}^0\cdot(\langle\boldsymbol{D}^{\sigma-1}\rangle\cdot\boldsymbol{D}^0 - 2\boldsymbol{I})\right)\cdot\nabla c^0\,|\Omega|\,. \tag{19}$$

The utility of these expressions is clear: *with knowledge of the uniform field, $\boldsymbol{D}^0$ and the volumetric quantities, $\langle\boldsymbol{D}^{\sigma}\rangle$ and $\langle\boldsymbol{D}^{\sigma-1}\rangle$, one can bound the deviation between the stress-free and stress-dependent solutions.* We now show that this bound collapses to very simple forms in special cases.

Special cases of $\boldsymbol{D}^{\sigma}$. For those cases having either type of uniform boundary conditions, with no body sources, it is straightforward to show that if $\langle\boldsymbol{D}^{\sigma}\rangle = \boldsymbol{D}^0$ (which does not imply, $\langle\boldsymbol{D}^{\sigma-1}\rangle = \boldsymbol{D}^{0-1}$), then inequality (19) collapses to

$$\|c^{\sigma} - c^{0}\|^2_{D^{\sigma}(\Omega)} \leq \mathcal{F}^0\cdot(\langle\boldsymbol{D}^{\sigma-1}\rangle - \langle\boldsymbol{D}^{\sigma}\rangle^{-1})\cdot\mathcal{F}^0\,|\Omega| = \mathcal{F}^0\cdot(\langle\boldsymbol{D}^{\sigma-1}\rangle - \boldsymbol{D}^{0-1})\cdot\mathcal{F}^0\,|\Omega|, \tag{20}$$

where $\mathcal{F}^0(=\boldsymbol{D}^0\nabla c^0)$ is the flux in the unstressed body.

If the lower bound is chosen $\langle\boldsymbol{D}^{\sigma-1}\rangle^{-1} = \boldsymbol{D}^0$ (which does not imply, $\langle\boldsymbol{D}^{\sigma}\rangle = \boldsymbol{D}^0$), then for either type of boundary condition, inequality (19) collapses to

$$\|c^{\sigma} - c^{0}\|^2_{D^{\sigma}(\Omega)} \leq \nabla c^0\cdot(\langle\boldsymbol{D}^{\sigma}\rangle - \langle\boldsymbol{D}^{\sigma-1}\rangle^{-1})\cdot\nabla c^0\,|\Omega| = \nabla c^0\cdot(\langle\boldsymbol{D}^{\sigma}\rangle - \boldsymbol{D}^0)\cdot\nabla c^0\,|\Omega|, \tag{21}$$

where $\nabla c^0(=\boldsymbol{D}^{0-1}\cdot\mathcal{F}^0)$ is the concentration gradient state that exists in the stress-free body. We observe that in both of these cases the difference in the classical bounds in Eq. (14) appear.

4.3 Diffusivities admitting a multiplicative decomposition

It is convenient to write the stress dependency of the diffusivity tensor as a multiplicative decomposition of the following form

$$\begin{aligned} &\mathcal{F} = -\boldsymbol{D}^{\sigma}(\boldsymbol{\sigma}) \cdot \nabla c, \\ &\boldsymbol{D}^{\sigma}(\boldsymbol{\sigma}) = \boldsymbol{H}(\boldsymbol{\sigma}) \cdot \boldsymbol{D}^{0}, \\ &\boldsymbol{H}(\boldsymbol{0}) = \boldsymbol{I}. \end{aligned} \tag{22}$$

It is required that the tensor function $\boldsymbol{H}(\boldsymbol{\sigma})$ has eigenvalues greater than 1 for a negative pressure (a *tensile* stress state), and eigenvalues less than one for a positive pressure (a *compressed* stress state). Essentially, this simple model captures the central *phenomenological* effect of the local volume changes – namely the enhancement or inhibition of diffusion by tensile and compressive stress states, respectively. If we consider cases where the multiplicative decomposition is possible, we have the following reduced form of the $\mathcal{B}_{(\sigma-0)}$-bounds for the general conditions and the special cases considered in the previous subsection:

$$\begin{aligned} &\mathcal{B}^2_{(\sigma-0)} = \int_{\Omega} (\boldsymbol{I} - \boldsymbol{H}(\boldsymbol{\sigma})^{-1}) \cdot \nabla c^0 \cdot (\boldsymbol{H}(\boldsymbol{\sigma}) \cdot \boldsymbol{D}^0) \cdot (\boldsymbol{I} - \boldsymbol{H}(\boldsymbol{\sigma})^{-1}) \cdot \nabla c^0 \, d\boldsymbol{x} \; (general), \\ &\mathcal{B}^2_{(\sigma-0)} = \nabla c^0 \cdot (\langle \boldsymbol{H}(\boldsymbol{\sigma}) \rangle + \langle \boldsymbol{H}(\boldsymbol{\sigma})^{-1} \rangle - 2\boldsymbol{I}) \cdot \mathcal{F}^0 \, |\Omega| \; (uniform), \\ &\mathcal{B}^2_{(\sigma-0)} = \nabla c^0 \cdot (\boldsymbol{I} - \langle \boldsymbol{H}(\boldsymbol{\sigma})^{-1} \rangle) \cdot \mathcal{F}^0 \, |\Omega| \; (uniform \; and \; \langle \boldsymbol{D}^{\sigma} \rangle = \boldsymbol{D}^0 \Longrightarrow \langle \boldsymbol{H}(\boldsymbol{\sigma}) \rangle = \boldsymbol{I}), \\ &\mathcal{B}^2_{(\sigma-0)} = \nabla c^0 \cdot (\langle \boldsymbol{H}(\boldsymbol{\sigma}) \rangle - \boldsymbol{I}) \cdot \mathcal{F}^0 \, |\Omega| \; (uniform \; and \; \langle \boldsymbol{D}^{\sigma-1} \rangle^{-1} = \boldsymbol{D}^0 \Longrightarrow \langle \boldsymbol{H}(\boldsymbol{\sigma})^{-1} \rangle = \boldsymbol{I}). \end{aligned} \tag{23}$$

We also see that, for the multiplicative decomposition, the bandwidth (Eq. (17)) of the effective property deviation collapses to

$$\boldsymbol{D}^0 \cdot \left(\langle \boldsymbol{H}(\boldsymbol{\sigma})^{-1} \rangle^{-1} - \boldsymbol{I} \right) \leq \boldsymbol{D}^{\sigma *} - \boldsymbol{D}^{0*} \leq \boldsymbol{D}^0 \cdot \left(\langle \boldsymbol{H}(\boldsymbol{\sigma}) \rangle - \boldsymbol{I} \right). \tag{24}$$

It is clear that the proximity of $\langle \boldsymbol{H}(\boldsymbol{\sigma}) \rangle$ to $\langle \boldsymbol{H}(\boldsymbol{\sigma})^{-1} \rangle^{-1}$ dictates the possible difference, due to stress, in the effective diffusivities, and the bound for the difference in the solution arising from stress.

5 Examples

We now pursue some quantitative examples. Thus far in the analysis, the bounds on the difference in diffusion solutions and effective properties have been derived for an arbitrary stress field. Obviously, there are a variety of possibilities to consider. In order to narrow the scope of the study, yet consider a wide range of possibilities, the two classical extreme elastic cases are used: (1) the Voigt Field, a uniform microstrain assumption, and (2) the Reuss Field, a uniform microstress assumption. The first produces statically inadmissible fields, while the second produces kinematically inadmissible fields. In a sense, the assumptions of the Reuss or Voigt fields provide the two extremes of expected elastic microfield behavior. We consider a unit cube of material with a heterogeneous elastic microstructure (Fig. 1) but with a constant, isotropic, diffusivity $\boldsymbol{D}^0$, i.e., the material *constituents* have different elastic properties, but the same (isotropic) diffusivity. A uniform specified boundary concentration is used, therefore c^0 is trivially computed analytically. We use the Reuss and Voigt pressure fields to produce the

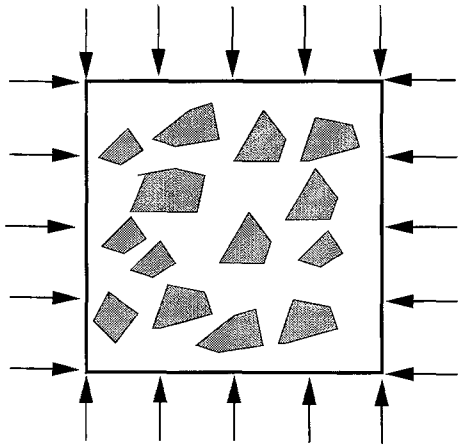

Fig. 1. A test problem (cross-section). Both uniform exterior compressive pressure and tensile pressure cases are considered

changes in diffusivity due to stress. Both tension and compression tests are performed. We track the two important qualities:

- The normalized predicted error:

$$NPE \stackrel{\text{def}}{=} \frac{\mathcal{B}_{(\sigma-0)}}{\|c^0\|_{D^0(\Omega)}} = \sqrt{\frac{\nabla c^0 \cdot \left(\boldsymbol{D}^0 \cdot \left(\langle \boldsymbol{H}(\boldsymbol{\sigma})\rangle + \langle \boldsymbol{H}(\boldsymbol{\sigma})^{-1}\rangle - 2\boldsymbol{I}\right)\right) \cdot \nabla c^0}{\nabla c^0 \cdot \boldsymbol{D}^0 \cdot \nabla c^0}} \tag{25}$$

- The normalized predicted effective property bandwidth:

$$NPEPB \stackrel{\text{def}}{=} \sqrt{\frac{\nabla c^0 \cdot \left(\boldsymbol{D}^0 \cdot \left(\langle \boldsymbol{H}(\boldsymbol{\sigma})\rangle - \langle \boldsymbol{H}(\boldsymbol{\sigma})^{-1}\rangle^{-1}\right)\right) \cdot \nabla c^0}{\nabla c^0 \cdot \boldsymbol{D}^0 \cdot \nabla c^0}} \tag{26}$$

5.1 Quantitative results

It is reasonable, in the context of small deformations, that only dilatational dependency is postulated, i.e., $\boldsymbol{D}^\sigma(\boldsymbol{\sigma}) = F(P)\boldsymbol{I} \cdot \boldsymbol{D}^0$, where P is the hydrostatic pressure ($= -tr\boldsymbol{\sigma}/3$). A very simple candidate to modify the diffusivity is

$$F(P) = (1 - sP) \qquad P = P(\boldsymbol{x}) \Longrightarrow \boldsymbol{D}^\sigma = (1 - sP)\,\boldsymbol{I} \cdot \boldsymbol{D}^0, \tag{27}$$

where s is a finite nonnegative constant parameter which depends on the temperature, the universal gas constant and the partial molar volume of the diffusing species. Of course there are restrictions on the combinations of s and $P(\boldsymbol{x})$, since $F(P)$ must remain positive. The extreme Reuss and Voigt pressure fields are respectively

$$P = P^R \qquad or \qquad P = P^V = P^R \frac{\varkappa}{\langle \varkappa \rangle}, \tag{28}$$

where $\varkappa$ is the spatially variable bulk modulus of the material. Obviously, if $\boldsymbol{D}^0$ is isotropic, the Reuss pressure field produces no change in the solution since it is constant, and simply scales out of the governing equations. Therefore only the Voigt field is of any interest in these examples. This choice of pressure field in Eq. (28) allows the same average pressure to be present in the system for the Reuss or Voigt fields, i.e.,

$$\int_\Omega P^R \, d\boldsymbol{x} = \int_\Omega P^V \, d\boldsymbol{x} = P^R. \tag{29}$$

For uniform concentration loading only volume fractions are needed in the computation of the bounds. For a two-phase heterogeneous material, using the simple functional value of $F(P)$, the averaged quantities needed become

$$\langle \boldsymbol{H}(\boldsymbol{\sigma}) \rangle = \langle F(P) \rangle \, \boldsymbol{I} = (1 - s\langle P \rangle) \, \boldsymbol{I} = (1 - sP^R) \, \boldsymbol{I},$$
$$\langle \boldsymbol{H}^{-1}(\boldsymbol{\sigma}) \rangle = \langle F^{-1}(P) \rangle \, \boldsymbol{I} = \left(\frac{VF}{1 - sP^R \dfrac{\varkappa_2}{\langle \varkappa \rangle}} + \frac{1 - VF}{1 - sP^R \dfrac{\varkappa_1}{\langle \varkappa \rangle}} \right) \boldsymbol{I}, \tag{30}$$

where $VF =$ volume fraction of the second phase and $\varkappa_1$ and $\varkappa_2$ are the bulk moduli of the first and second phases respectively.

5.1 Observations

Figures 2–11 illustrate results for a sample of a two-phase composite material shown in Fig. 1 under uniform external pressure. Of course the internal fields are highly variable. Both compression and tension tests are performed. The bounds on the difference in the stress-free and stress-assisted diffusion models, and the bandwidth for the effective property deviation, are depicted. Since volume fractions only are needed in the computation of the bound for the solution difference and of the effective property bandwidth, the actual microstructural topology is general. Also since pressure dependence of the form in Eq. (28) is used, the only other parameter needed is the mismatch in elastic bulk properties $\tau \overset{\text{def}}{=} \varkappa_2/\varkappa_1$. In order to avoid absurd behaviour (i.e., "negative diffusion") we must require $\max_{x \in \Omega} |sP(\boldsymbol{x})| < 1$. To be consistent we do this for both the compression and tension tests. Accordingly, in these tests we choose $s = 1$ and vary τ, P^R and VF.

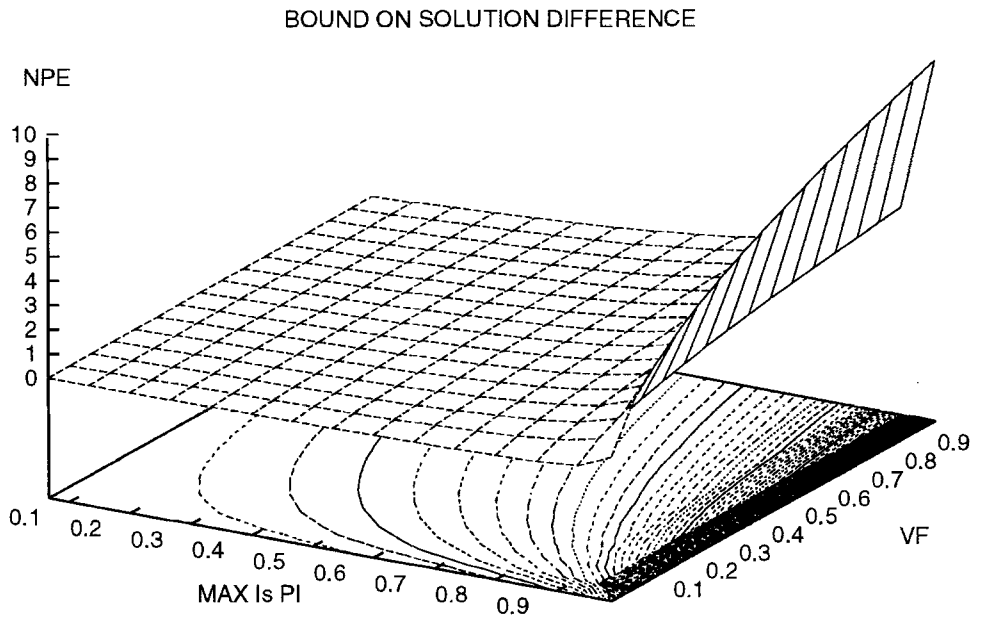

Fig. 2. (Compression test) The behavior of the NPE for $\tau = 10$. The iso-value contours are projected on the base of the plot.

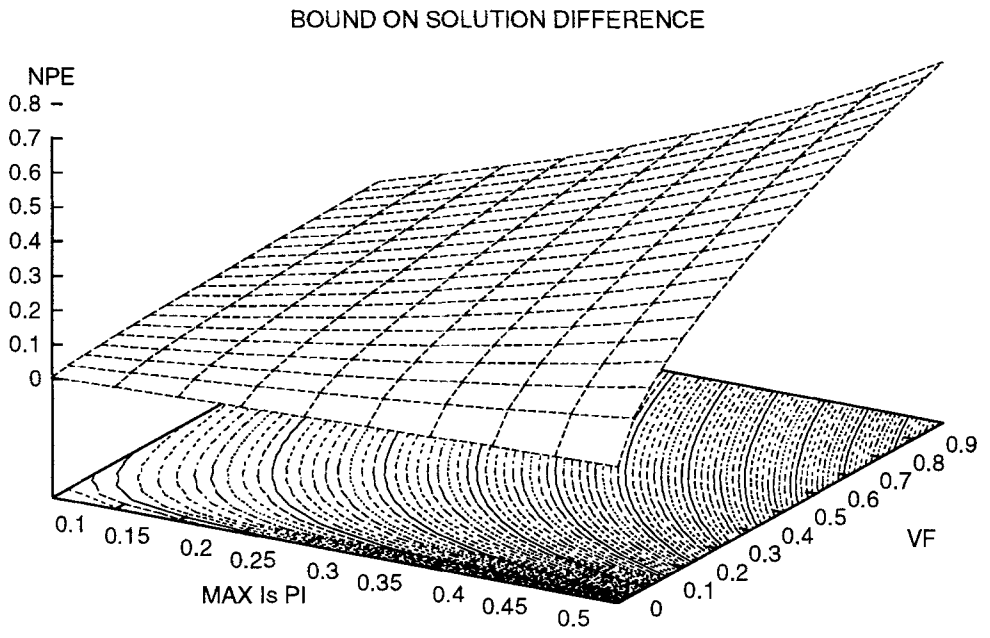

Fig. 3. (Compression test) A closeup view for lower volume fractions. The behavior of the NPE for $\tau = 10$

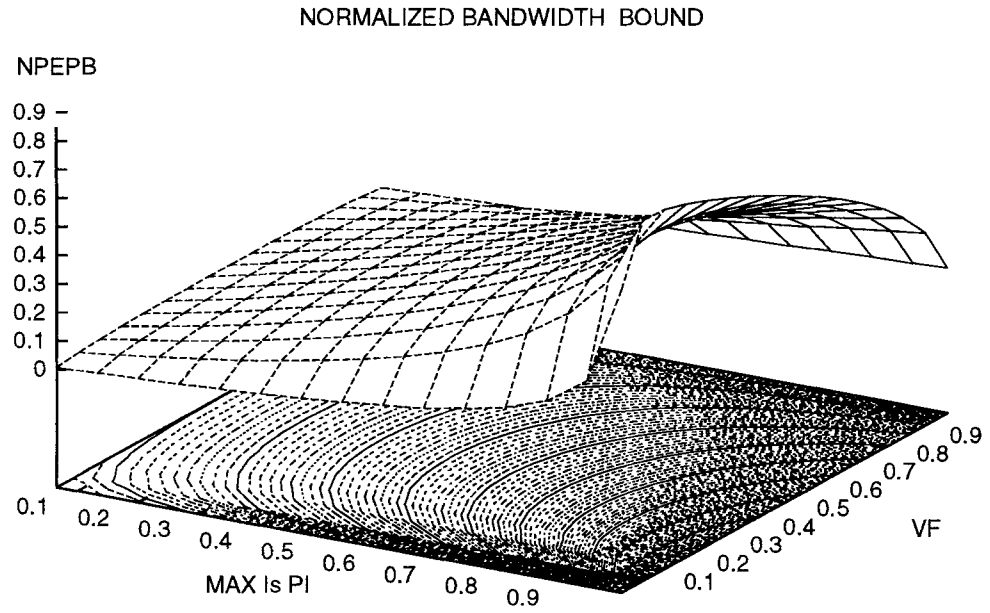

Fig. 4. (Compression test) The behavior of the $NPEPB$ for $\tau = 10$

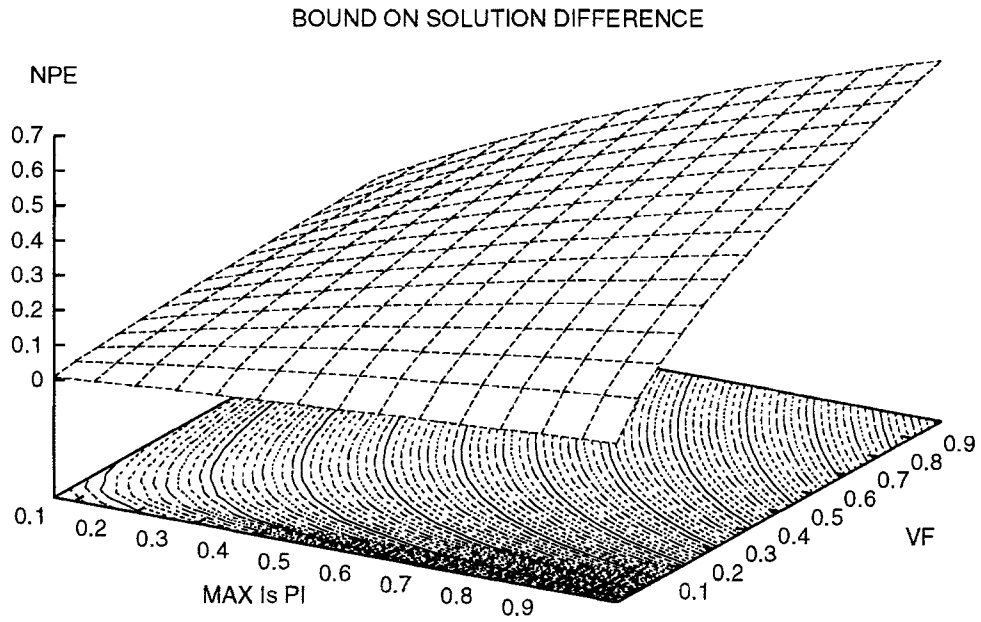

Fig. 5. (Tension test) The behavior of the NPE for $\tau = 10$

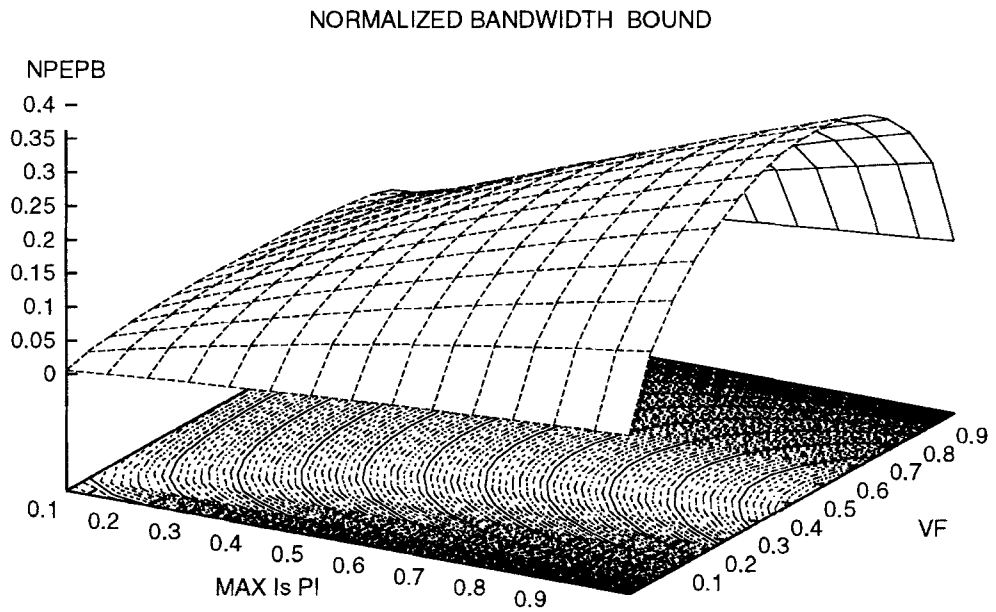

Fig. 6. (Tension test) The behavior of the $NPEPB$ for $\tau = 10$

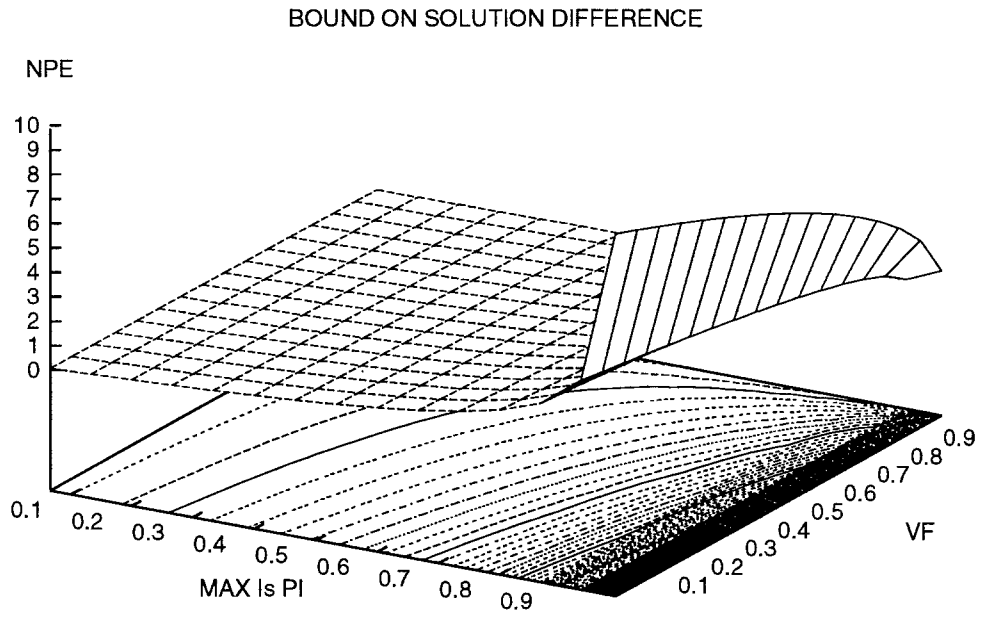

Fig. 7. (Compression test) The behavior of the NPE for $\tau = 0.1$

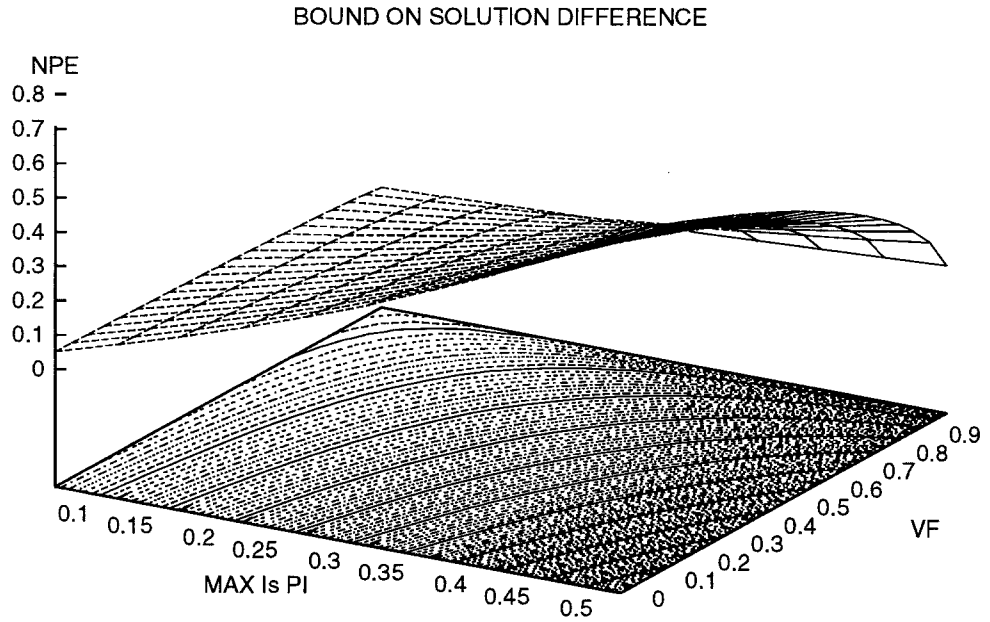

Fig. 8. (Compression test) A closeup view for lower volume fractions. The behavior of the NPE for $\tau = 0.1$

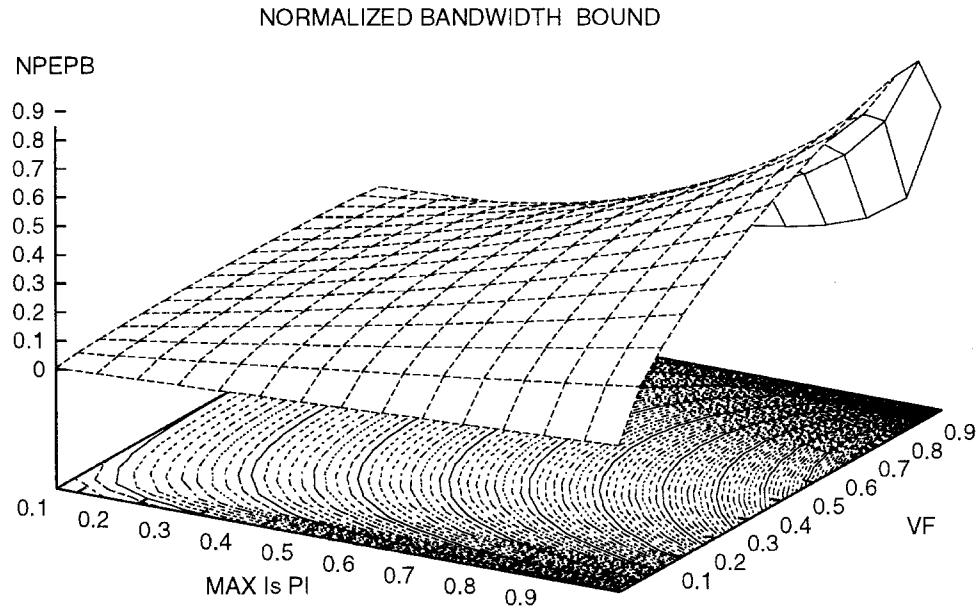

Fig. 9. (Compression test) The behavior of the $NPEPB$ for $\tau = 0.1$

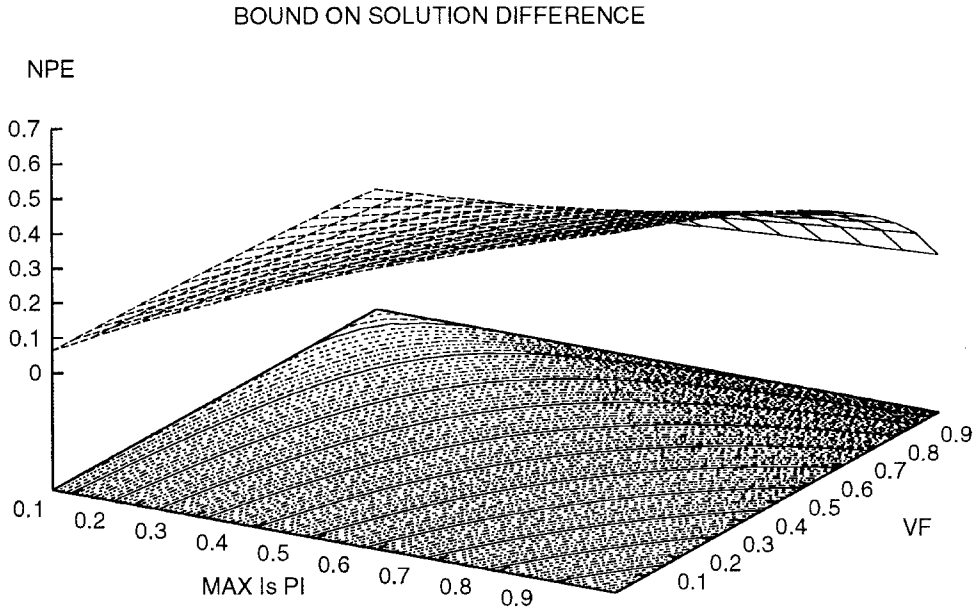

Fig. 10. (Tension test) The behavior of the NPE for $\tau = 0.1$

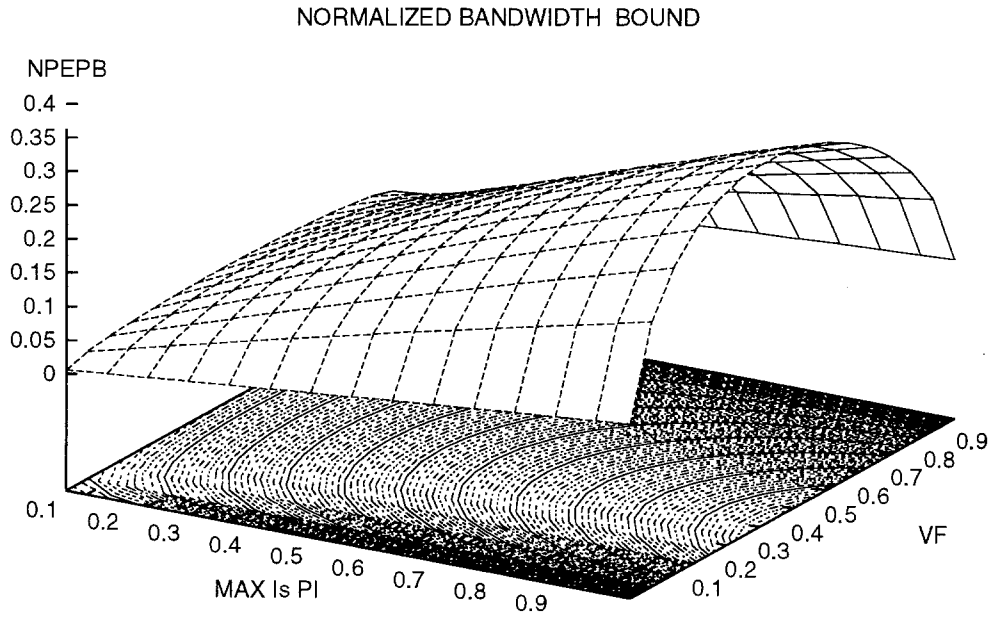

Fig. 11. (Tension test) The behavior of the $NPEPB$ for $\tau = 0.1$

Obviously large differences in the solutions result which different microstructures and pressure loading. As seen in Fig. 2–11, the normalized predicted error between the stress-dependent solution and the stress-free solution, NPE, can be several hundred percent in the compressive case. The normalized predicted effective property bandwidth, NPEPB, of the deviation of effective properties, is also significant, if not quite as dramatically so. As illustrated in the numerical experiments, differences in the stress-dependent and stress-free solutions and the deviation of effective properties grow monotonically with pressure. The differences in the stress-dependent and stress-free solutions also grow monotonically with volume fraction. Of course this is not the case with the deviation in effective properties which must tend to zero for both extremes, $VF = 0$ and $VF = 1$. For this example, the behavior of the effective properties and the deviation in the solution fields behave differently with respect to volume fraction changes. NPE tends to a finite number at either extreme volume fraction due to the restriction $\max_{x \in \Omega} |sP(\boldsymbol{x})| < 1$.

6 Conclusion

In concluding this paper, the main point which we wish to emphasize is that the bounds provide a way of determining when stress may play an important role in the diffusion process. We have attempted to illustrate this with as simple a model as possible. The magnitude of the bounds can be used to decide whether an expensive set of calculations, possibly involving numerical or laboratory experiments, is necessary. It is a certainty that, for virtually every possible external loading, the internal stress fields are not uniform due to heterogeneities on the microscale. Hence the bounds provide a means of quantitatively and qualitatively deter-

mining the effects of nonuniform stress in solid state diffusion. The general form of the solution deviation bound is valid for arbitrary microstructures, loading and external geometry, and requires knowledge of the stress field and the stress-free solution. *It does not require any knowledge of the behavior of the stress-dependent solution, which is in general extremely expensive to compute.* For example with the finite element or finite difference method, the distance between discretization nodes must be far smaller than the microstructural oscillations to obtain accurate simulations, thus making a direct numerical simulation of this class of problems virtually impossible without special techniques. Therefore, the bound can be used to determine whether such calculations are needed. The various forms of the bound can be used to provide a measure of the error in using a simpler, and relatively inexpensive, model for diffusion in the presence of stress. However, judging from the examples given in this paper, in some cases, the effects of stress may be significant enough to warrant potentially expensive numerical simulations.

Acknowledgements

The authors wish to thank the anonymous reviewers for their constructive comments.

References

[1] Gerberich, W. W., Livne, T., Chen, X. F., Kaczorowski, M.: Crack growth from hydrogen-temperature and microstructural effects in 4340 steel. Metall. Trans. **19A,** 1319–1334 (1988).
[2] Gerberich, W. W., Foecke, T. J.: Hydrogen enhanced decohesion in Fe-Si single crystal. In: Implications to modeling thresholds in hydrogen effects on material behavior (Moody, N. R., Thompson, A. W., eds.), pp. 687–702. The Minerals, Metals and Materials Society 1990.
[3] Van der Burg, M. W. D., Van der Giessen, E., Brouwer, R. C.: Investigation of hydrogen attack in 2.25Cr-1Mo steels with a high-triaxiality void growth model. Acta Metall. **44,** 505–518 (1996).
[4] Metals Handbook (Leiter, R. et al. eds.): Failure analysis and prevention, vol. 2, 8th ed., Ohio: The American Society for Metals 1975.
[5] Maxwell, J. C.: On the dynamical theory of gases. Philo. Trans. Soc. London **157,** 49 (1867).
[6] Joseph, D. D., Preziosi, L.: Heat waves. Rev. Mod. Phys. **61,** (1) 41–73 (1989).
[7] Jou, D., Casas-Vazqzez, J., Lebon, G.: Extended irreversible thermodynamics. Rep. Prog. Phys. **51,** 1105–1179 (1988).
[8] Dreyer, W., Struchtrup, H.: Heat pulse experiments revisited. Cont. Mech. Thermodyn. **5,** 3–50 (1993).
[9] Chandrasekhariah, D. S.: Thermoelasticity with second sound: a review. Appl. Mech. Rev. **39,** 355–376 (1986).
[10] Muller, I., Ruggeri, T.: Extended thermodynamics. New York: Springer 1993.
[11] Crank, J.: The mathematics of diffusion, 2nd ed., Oxford: Oxford Science Publications 1975.
[12] Aifantis, D. C.: New interpretation of diffusion in regions with high diffusivity paths: A continuum approach. Acta Metall. **27,** 683–691 (1979).
[13] Doig, P., Jones, T. A.: Model for the initiation of hydrogen embrittlement cracking at notches in gaseous hydrogen environments. Metall. Trans. **18A,** 1993–1998 (1977).
[14] Unger, D. J., Aifantis, D. C.: On the theory of stress-assisted diffusion, part II. Acta Mech. **47,** 117–151 (1983).
[15] Unger, D. J., Gerberich, W. W., Aifantis, D. C.: Further remarks on the implications of steady-state stress-assisted diffusion on environmental cracking. Scripta Metall. **16,** 1059–1064 (1982).
[16] Van Leeuwen, H. P.: A quantitative model of hydrogen induced grain boundary cracking. Corrosion **29,** 197–204 (1973).

[17] Hashin, Z.: Analysis of composite materials: a survey. J. Appl. Mech. **50,** 481–505 (1983).
[18] Aifantis, E. C.: Some remarks concerning the solid-state diffusivity tensor. In: Proceedings of the Sixth Canadian Congress of Applied Mechanics, pp. 957–958. Vancouver: University of British Columbia Press 1977.
[19] Flynn, C. P.: Point defects and diffusion. Oxford: Clarendon Press 1972.
[20] Voigt; W.: Über die Beziehung zwischen den beiden Elastizitätskonstanten isotroper Körper. Wied. Ann. **38,** 573–587 (1889).
[21] Reuss, A.: Berechnung der Fließgrenze von Mischkristallen auf Grund der Plastizitätsbedingung für Einkristalle. ZAMM **9,** 49–58 (1929).
[22] Hill, R.: The elastic behaviour of a crystalline aggregate. Proc. Phys. Soc. London **A65,** 349–354 (1952).

Author's address: T. I. Zohdi and P. Wriggers, Institut für Baumechanik und Numerische Mechanik, Appelstrasse 9A, D-30167 Hannover, Germany